Vol 14 No 8, August 2005
1009-1963/2005/14(08)/1594-06

Chinese Physics

© 2005 Chin. Phys. Soc.
and IOP Publishing Ltd

Nonlinear propagation of focused ultrasound in layered biological tissues based on angular spectrum approach*

Zhu Xiao-Feng(朱晓峰), Zhou Lin(周 琳),
Zhang Dong(章 东)†, and Gong Xiu-Fen(龚秀芬)

State Key Laboratory of Modern Acoustics, Institute of Acoustics, Nanjing University, Nanjing 210093, China

(Received 14 December 2004; revised manuscript received 14 January 2005)

Nonlinear propagation of focused ultrasound in layered biological tissues is theoretically studied by using the angular spectrum approach (ASA), in which an acoustic wave is decomposed into its angular spectrum, and the distribution of nonlinear acoustic fields is calculated in arbitrary planes normal to the acoustic axis. Several biological tissues are used as specimens inserted into the focusing region illuminated by a focused piston source. The second harmonic components within or beyond the biological specimens are numerically calculated. Validity of the theoretical model is examined by measurements. This approach employing the fast Fourier transformation gives a clear visualization of the focused ultrasound, which is helpful for nonlinear ultrasonic imaging.

Keywords: Focused ultrasound, second harmonic imaging, angular spectrum approach
PACC: 4335, 8750C

1. Introduction

Ultrasonic imaging techniques have been widely used in medical diagnosis because they can provide important information on the diseased state of the tissues in a human body non-invasively and nondestructively. Such techniques are normally based on linear acoustical theory on sound propagation in tissues. However, many reports have indicated that the nonlinear acoustical effects should be considered in the range of biomedical frequencies and intensities.[1−3] Due to these nonlinear effects, a monochromatic sound wave will be distorted progressively and harmonics will be generated. Considering that the second harmonics has a good directional performance and spatial resolution compared with the fundamental frequency wave, the most current B-scanning has the function of the second harmonic imaging.[4−6] To improve the accuracy of the present imaging techniques and also explore new imaging techniques, we need to have a full knowledge of acoustic nonlinear generation in layered biological tissues. A theoretical model to describe the second harmonic generation in multi-layer media by using the superposition technique of Gaussian beams has been developed in our previous work.[7] Considering the diffraction effect due to the finite size of the transmitter, the second harmonic component can be described as a linear summation of self- and cross-interactions of the Gaussian beams. Although the technique is an effective tool to calculate the second harmonic generation in tissues, an axial symmetrical source and regular interfaces are needed.

The decomposition of an acoustic wave into its angular spectrum representation creates an effective base for the calculation of wave propagation effects in media. This approach employing the fast Fourier transformation is especially suitable for the visualization of the sound beam, which is helpful for ultrasonic imaging. In addition, the approach is suitable for arbitrary sound source and irregular interfaces. Using the angular spectrum approach (ASA), we studied the linear sound field in layered media, and derived an expression for an optimal selection of the angular range.[8] Alais and Hennion firstly introduced this technique into nonlinear acoustics to describe the sum and difference frequency components generated by a

*Project supported by the National Natural Science Foundation of China (Grant No 10204014).
†E-mail: dzhang@nju.edu.cn

parametric acoustic array.[9] Landsberger and Hamilton investigated nonlinear generation from a planar source in solid materials by using the ASA.[10] In this paper, we apply this approach to the investigation into the second harmonic generation in biological tissues from a piston focusing source, and the visualization of the nonlinear ultrasonic beam in the focusing region. Validity of the numerical calculation is examined by the measurements for several biological tissues.

2. Principle and method

2.1. Harmonic generation in the region before the specimen

As shown in Fig.1, a uniformly excited focusing source with a radius a and focusing length D is employed as the transmitter. A biological tissue specimen with a thickness d is inserted into the focusing

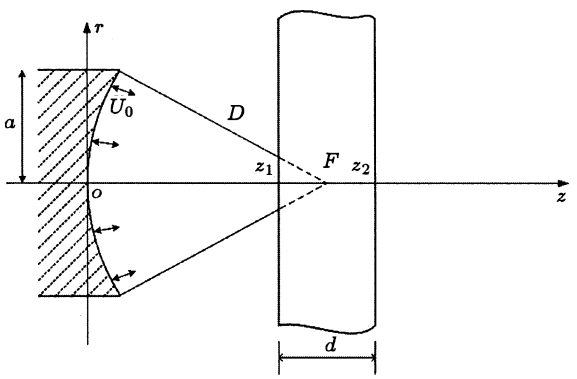


Fig.1. Illustration of focused acoustic source.

region. It is well known that when a finite-amplitude sound-wave is transmitted in a medium, the wave distortion will occur and higher harmonics are accumulated during its propagation due to the nonlinearity of the medium. The nonlinear sound propagation satisfies the following nonlinear equation[11]:

$$\left(\nabla^2 - \frac{1}{c^2}\frac{\partial^2}{\partial t^2}\right) p = -\frac{\beta}{\rho c^4}\frac{\partial^2 p^2}{\partial t^2}, \tag{1}$$

where ∇ is the Laplace operator, ρ and c are density and velocity respectively, p refers to the sound pressure, β is the coefficient of nonlinearity, $\beta = 1 + B/2A$, B/A denotes the acoustic nonlinearity parameter, which is used to present the nonlinearity effect produced during the sound propagation in a medium.[12] In a quasi-linear approximation, the sound pressure p can be expressed as follows:

$$p = p_1 + p_2, \tag{2}$$

where p_1 and p_2 denote the fundamental and second-harmonic components respectively. We let

$$p_n(x, y, z, t) = P_n(x, y, z)e^{-\mathrm{j}n\omega t}, \tag{3}$$

where ω is the angular frequency, and $n = 1, 2$. By substituting Eqs.(2) and (3) into Eq.(1), we obtain

$$(\nabla^2 + k^2)P_1 = 0, \tag{4}$$

$$\begin{aligned}(\nabla^2 + 4k^2)P_2 = &\frac{2\beta k^2}{(2\pi)^4 \rho c^2} \iiiint \mathrm{e}^{\mathrm{j}(k'+k'')\cdot r} \\ &\times \hat{P}_1(k'_x, k'_y, z_0) \\ &\times \hat{P}_1(k'_x, k'_y, z_0)\mathrm{d}k'_x \mathrm{d}k'_y \mathrm{d}k''_x \mathrm{d}k''_y, \end{aligned} \tag{5}$$

where $k = \omega/c$. Suppose that the sound wave travelling in the positive z-axis is incident on the xy plane, decomposition of the source plane can be done in the sense of a transformation from the space vector domain to the spatial frequencies domain. If the source spectrum is given in the plane $z = 0$ by

$$\widehat{P}_1(k_x, k_y, 0) = \mathbf{F}\{P_1(x, y, 0)\}, \tag{6}$$

where $\mathbf{F}\{\}$ represents the Fourier transformation. k_x and k_y are wave numbers in planes parallel to the source plane. Then the solution of Eq.(4) for the fundamental frequency wave in the plane $z = z_1$ is

$$P_1(x, y, z_1) = \mathbf{F}^{-1}\{\hat{P}_1(k_x, k_y, 0)\mathrm{e}^{\mathrm{j}k_z z_1}\}, \tag{7}$$

where $\mathbf{F}^{-1}\{\}$represents the inverse Fourier transformation. $k_z = \sqrt{k^2 - k_x^2 - k_y^2}$ is the wave number in planes perpendicular to the source plane. Substituting Eq.(7) into Eq.(5) yields the solution for the second harmonic component in the plane $z = z_1$ as follows:

$$\begin{aligned}\hat{P}_2(k_x, k_y, z_1) = &\iint Q_f(k_x, k_y, k'_x, k'_y, z_1)\hat{P}_1(k'_x, k'_y, 0) \\ &\times \hat{P}_1(k_x - k'_x, k_y - k'_y, 0)\mathrm{d}k'_x \mathrm{d}k'_y, \end{aligned} \tag{8}$$

where

$$Q_\mathrm{f}(k_x, k_y, k'_x, k'_y, z_1) = \frac{2\beta k^2}{\rho c^2}\left(\frac{\mathrm{e}^{\mathrm{i}(k''_z + k'_z)z_1} - \mathrm{e}^{\mathrm{i}k_{2z}z_1}}{k_{2z}^2 - (k''_z + k'_z)^2}\right),$$

and

$$\begin{aligned} k'_z &= \sqrt{k^2 - (k'_x)^2 - (k'_y)^2}, \\ k''_z &= \sqrt{k^2 - (k_x - k'_x)^2 - (k_y - k'_y)^2}, \\ k_{2z} &= \sqrt{(2k)^2 - k_x^2 - k_y^2}. \end{aligned}$$

Considering the sound attenuation in an *ad hoc* manner, k_z,k'_z and k_{2z} may be substituted respectively

by $\tilde{k}_z$, $\tilde{k}'_z$ and $\tilde{k}_{2z}$ which are defined as $\tilde{k}_z = k_z + \mathrm{j}\frac{k}{k_z}\alpha_1$, $\tilde{k}'_z = k'_z + \mathrm{j}\frac{k}{k'_z}\alpha_1$ and $\tilde{k}_{2z} = k_{2z} + \mathrm{j}\frac{k}{k_{2z}}\alpha_2$. α_1 and α_2 are the sound attenuation coefficients at the fundamental and second harmonic frequencies, respectively.

2.2. Harmonic generation within and beyond the specimen

To deal with the sound transmission in multi-layer media, we ignore the sound reflection due to a small difference in sound impedance between water and biological tissues. The transmission coefficient of sound pressure T at the interface $z = z_1$ can be expressed as[8]

$$T = \frac{2\rho_{\mathrm{s}} c_{\mathrm{s}} \sqrt{1-(\lambda k_x/2\pi)^2-(\lambda k_y/2\pi)^2}}{\rho_{\mathrm{s}} c_{\mathrm{s}} \sqrt{1-(\lambda k_x/2\pi)^2-(\lambda k_y/2\pi)^2} + \rho_A c_A \sqrt{1-(\lambda_{\mathrm{s}} k_{sx}/2\pi)^2-(\lambda_{\mathrm{s}} k_{sy}/2\pi)^2}}, \tag{9}$$

where the parameters denoted by the subscript "s" are for the tissue sample. The angular spectra in the specimen at the plane $z = z_1$ are given by

$$\hat{P}_1(k_{sx}, k_{sy}, z_1) = T\hat{P}_1(k_x, k_y, z_1), \tag{10}$$

$$\hat{P}_2(k_{sx}, k_{sy}, z_1) = T\hat{P}_2(k_x, k_y, z_1). \tag{11}$$

The second harmonic component in the plane $z = z_2$ is composed of two parts: one of them results from $P_2(x, y, z_1)$ by linear propagation, and the other is nonlinearly generated from $P_1(x, y, z_1)$. Hence the angular spectrum of the second harmonic component in the plane $z = z_2$ is

$$\begin{aligned}\hat{P}_2(k_x, k_y, z_2) = \iint & Q_{\mathrm{sf}}(k_{sx}, k_{sy}, k'_{sx}, k'_{sy}, z) \\ & \times \hat{P}_1(k'_{sx}, k'_{sy}, z_1) \\ & \times \hat{P}_1(k_{sx}-k'_{sx}, k_{sy}-k'_{sy}, z_1)\mathrm{d}k'_x\mathrm{d}k'_y \\ & + \hat{P}_2(k_{sx}, k_{sy}, z_1)\mathrm{e}^{\mathrm{j}k_{2z}z},\end{aligned} \tag{12}$$

where

$$\begin{aligned}& Q_{\mathrm{sf}}(k_{sx}, k_{sy}, k'_{sx}, k'_{sy}, z) \\ =& \frac{2\beta_{\mathrm{s}} k_{\mathrm{s}}^2}{\rho_{\mathrm{s}} c_{\mathrm{s}}^2}\left(\frac{\mathrm{e}^{\mathrm{i}(k''_z+k'_z)z} - \mathrm{e}^{\mathrm{i}k_{2z}z}}{k_{2z}^2-(k''_z+k'_z)^2}\right).\end{aligned} \tag{13}$$

For the region $z > z_2$, the angular spectrum of the second harmonic component can be obtained by using the similar process to that in the plane $z = z_2$.

3. Experimental system

The basic scheme of the measurement set-up is demonstrated in Fig.2. A programmable function generator (Agilent 33250, USA) transmits a repeated tone-burst signal containing 10 cycles of the fundamental sine wave (5MHz) with an amplitude of 60mV and a repetition frequency of 1kHz; it is long enough to be treated as a continuous wave, yet short enough to eliminate the standing wave effect within the holder of the specimen. The emitted tone-burst signal is amplified by a broadband power amplifier (ENI A-150, USA) and used to drive a focused transmitter with a resonance frequency of 5MHz, a diameter of 8mm, and a focusing length of 51mm. The acoustic signal after propagating through the specimen is detected by a broadband needle hydrophone (NTR1000, USA). Finally, the received signal is amplified and sent to a digital oscilloscope (Agilent 54831, USA) for its digitizing and finally stored in the computer.

To measure the two-dimensional distribution of sound radiated from the focused transducer, the hydrophone is mounted on a two-dimensional mechanical scanning unit (Newport MM3000, USA). Using this scanning system, the data are sampled at an interval of 0.05mm in the plane normal to the acoustic axis. The scanning region is 20mm×20mm, hence, a matrix of 400×400 is obtained to visualize the second harmonic distribution.

Several biological tissues are used as the specimens in the measurement, including porcine fatty and liver tissues, and fresh eggs. The porcine fatty and liver tissues are obtained from a slaughter-house and stored in the physiological saline. All measurements are finished within 4 hours at a temperature of 25°C. The specimen is packed into a plexiglass cylindrical holder with two sound permeable planar membranes at both ends, and inserted into the focusing region. The dimension of the sample holder along the direction of acoustic axis is d=10mm.

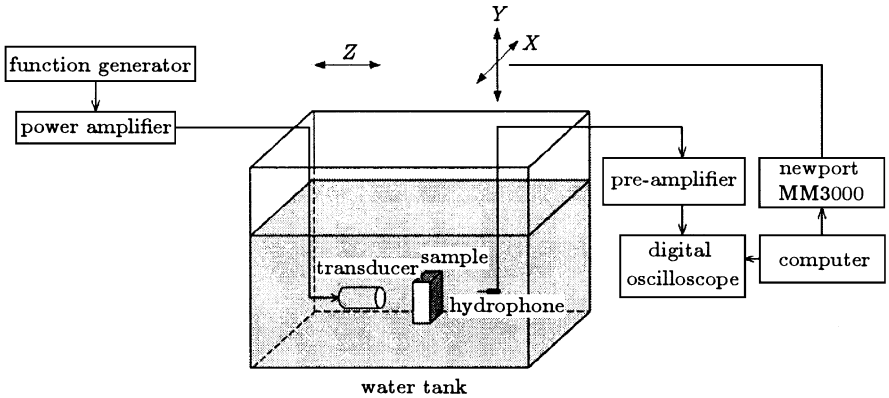


Fig.2. Block-diagram of the experimental system.

4. Comparison between numerical calculation and measured results

In the numerical calculation, the first set of computations is based on discretization of source plane, in which the sampling interval δ must satisfy the Nyquist sampling theorem ($\delta \leq \lambda/2$). In addition, to reduce the aliasing error due to the circular convolution, the sampling region should be larger than the area of the source. Therefore, the sample interval δ=0.1mm is chosen to discrete the rectangular region (10mm×10mm) in the source plane. The normal velocity on the surface of the transmitter is

$$u(x,y,0) = \frac{u_0}{\mathrm{i}k}\exp\left(-\frac{\mathrm{i}kr^2}{2D}\right), \quad r < a,$$
$$u(x,y,0) = 0, \quad r > a. \tag{14}$$

Ultrasonic parameters of biological specimens are measured by the finite amplitude insert substitution technique[13] and listed in Table 1.

Table 1. Ultrasonic parameters for water and biological specimen.

Specimen	Density/(g/cm^3)	Velocity/(m/s)	Attenuation at 5MHz/(dB/cm)	Attenuation at 10MHz/(dB/cm)	β
Water	0.997	1497	0.5375	2.19	3.6[2]
Liver	1.05	1580	38.5	77.0	4.45
Fat	0.95	1445	119.25	238.5	6.45
White	1.033	1542	13.5	31.0	3.70
Yolk	1.066	1508	48.2	136.3	5.25

Solid lines in Figs.3 and 4 show the calculated second harmonic sound pressure distributions in the plane z=0.102m when the porcine fatty or liver tissue with the thickness d=0.01m is inserted into the focusing region, where the vertical axis is the axis normalized by the second harmonic sound pressure at z=0.102m without insertion of the specimen. To examine the validity of the ASA technique, we also give the corresponding measured results as shown in Figs.3 and 4 by dotted lines.

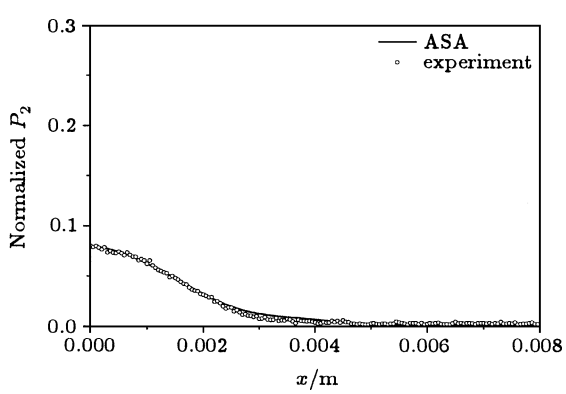


Fig.3. Comparison of beam pattern for the second harmonic component at z=0.102m between the prediction with ASA and the measurement with insertion of fat tissue.

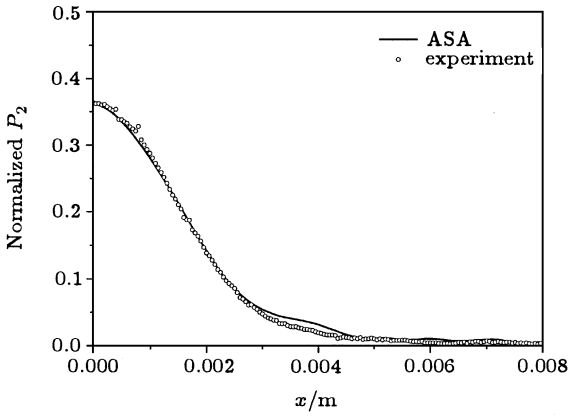


Fig.4. Comparison of beam pattern for the second harmonic component at z=0.102m between the prediction with ASA and the measurement with insertion of liver tissue.

Figure 5 demonstrates a comparison of the normalized beam pattern at z=0.102m with insertion of egg white and egg yolk in the focusing region between the prediction with ASA technique and the measurement, where the vertical axis is the axis normalized by the second harmonic sound pressure at z=0.102m without insertion of the specimen.

Agreement of the prediction by the ASA with the measurement shown in Figs.4 and 5 verifies the validity of the theoretical method. Therefore, we can predict the second harmonic sound distribution within the region of tissue specimen. Figure 6 gives planar scans of the second harmonic sound distribution in the focusing plane with the insertion of liver and fatty tissue. The vertical axis represents the normalized second harmonic pressure compared with that in pure water at z=0.051m. In the figure, it is easy to locate the convergence of the nonlinear sound beam in the focusing region, which is helpful to improve the resolution of nonlinear image.

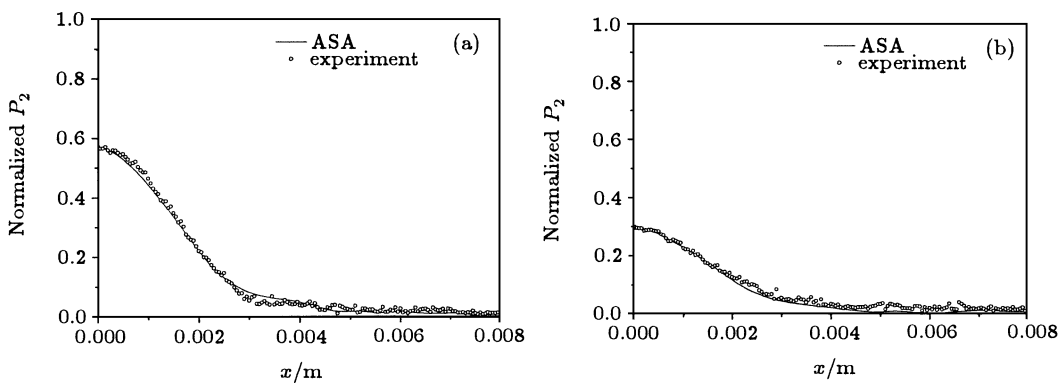


Fig.5. Comparison of beam pattern for the second harmonic component at z=0.102m between the prediction with ASA and the measurement with insertion of (a) egg white and (b) egg yolk.

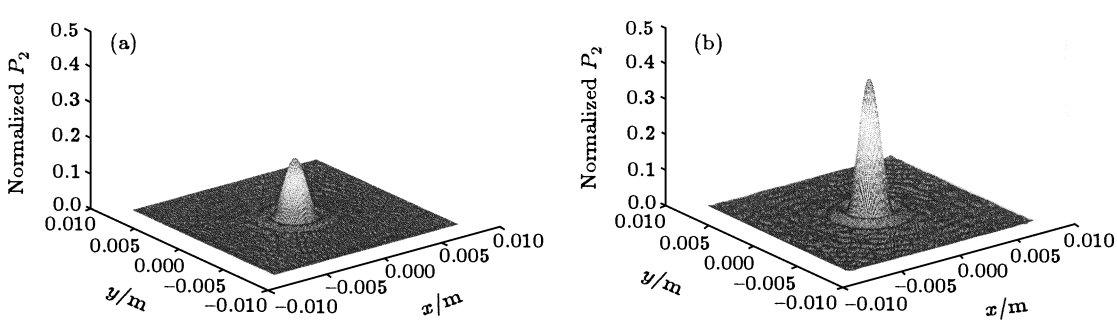


Fig.6. Planar scans in biological tissue at the plane z=0.051m (a) Fat (b) Liver.

5. Discussions and conclusion

In this paper, we study the second harmonic sound propagation in layered biological tissues illuminated by a focused piston transducer in theory as well as in measurement. Several biological tissues, including porcine fatty and liver tissue, egg white and egg yolk, are used as the specimens inserted into the focusing region. The planar scans of the second harmonic

sound distributions beyond the focusing region are theoretically predicted by using the angular spectrum approach, and in good agreement with the measurement. Therefore, we can predict the second harmonic sound distribution within the tissue specimens with the ASA technique, which could give helpful knowledge for the second harmonic imaging of tissue.

References

[1] Muir T G and Carstensen E L 1980 *Ultrasound in Med. Biol.* **6** 345

[2] Duck F A 2002 *Ultrasound in Med. Biol.* **28** 1

[3] Carstensen E L, Law W K, Mckay N D and Muir T G 1982 *Ultrasound in Med. Biol.* **6** 359

[4] Fatemi M and Greenleaf J F 1996 *Ultrasound in Med. Biol.* **22** 1215

[5] Puls I, Berg D, Maurer M, Schliesser M, Hetzel G and Becker G 2000 *Ultrasound in Med. Biol.* **26** 189

[6] Tanaka S, Oshikawa O, Sasaki T, Ioka T and Tsukuma H 2000 *Ultrasound in Med. Biol.* **26** 183

[7] Zhang D, Gong X F and Zhang B 2002 *J. Acoust. Soc. Am.* **111** 45

[8] Zhang W Y, Ye S G and Gong X F 1999 *Acta Phys. Sin.* **8** S63

[9] Alais P and Hennion P Y 1979 *Acustica* **43** 1

[10] Landsberger B J and Hamilton M F 2001 *J. Acoust. Soc. Am.* **109** 488

[11] Tjϕtta J N and Tjϕtta S 1987 *J. Acoust. Soc. Am.* **82** 1425

[12] Beyer R T 1960 *J. Acoust. Soc. Am.* **32** 719

[13] Gong X F, Zhu Z M, Shi T and Huang J H 1989 *J. Acoust. Soc. Am.* **86** 1